AFRL-RY-WP-TR-2013-0059

DESIGN AND FABRICATION OF A RADIO FREQUENCY GRIN LENS USING 3D PRINTING TECHNOLOGY

Jeffrey W. Allen and Bae-Ian Wu

Antennas & Electromagnetics Technology Branch
Multispectral Sensing & Detection Division

APRIL 2013
Final Report

STINFO COPY

AIR FORCE RESEARCH LABORATORY
SENSORS DIRECTORATE
WRIGHT-PATTERSON AIR FORCE BASE, OH 45433-7304
AIR FORCE MATERIEL COMMAND
UNITED STATES AIR FORCE

REPORT DOCUMENTATION PAGE

The public reporting burden for this collection of information is estimated to average 1 hour per response, including the time for reviewing instructions, searching existing data sources, gathering and maintaining the data needed, and completing and reviewing the collection of information. Send comments regarding this burden estimate or any other aspect of this collection of information, including suggestions for reducing this burden, to Department of Defense, Washington Headquarters Services, Directorate for Information Operations and Reports (0704-0188), 1215 Jefferson Davis Highway, Suite 1204, Arlington, VA 22202-4302. Respondents should be aware that notwithstanding any other provision of law, no person shall be subject to any penalty for failing to comply with a collection of information if it does not display a currently valid OMB control number. **PLEASE DO NOT RETURN YOUR FORM TO THE ABOVE ADDRESS**.

1. REPORT DATE *(DD-MM-YY)*	2. REPORT TYPE	3. DATES COVERED *(From - To)*
April 2013	Final	1 March 2012 – 1 March 2013

4. TITLE AND SUBTITLE
DESIGN AND FABRICATION OF A RADIO FREQUENCY GRIN LENS USING 3D PRINTING TECHNOLOGY

5a. CONTRACT NUMBER
In-house

5b. GRANT NUMBER

5c. PROGRAM ELEMENT NUMBER
N/A

6. AUTHOR(S)
Jeffrey W. Allen and Bae-Ian Wu (AFRL/RYMH)

5d. PROJECT NUMBER
N/A

5e. TASK NUMBER
N/A

5f. WORK UNIT NUMBER
N/A

7. PERFORMING ORGANIZATION NAME(S) AND ADDRESS(ES)
Antennas & Electromagnetics Technology Branch
Multispectral Sensing & Detection Division
Air Force Research Laboratory, Sensors Directorate
Wright-Patterson Air Force Base, OH 45433-7320
Air Force Materiel Command, United States Air Force

8. PERFORMING ORGANIZATION REPORT NUMBER
AFRL-RY-WP-TR-2013-0059

9. SPONSORING/MONITORING AGENCY NAME(S) AND ADDRESS(ES)
Air Force Research Laboratory
Sensors Directorate
Wright-Patterson Air Force Base, OH 45433-7320
Air Force Materiel Command
United States Air Force

10. SPONSORING/MONITORING AGENCY ACRONYM(S)
AFRL/RYMH

11. SPONSORING/MONITORING AGENCY REPORT NUMBER(S)
AFRL-RY-WP-TR-2013-0059

12. DISTRIBUTION/AVAILABILITY STATEMENT
Approved for public release; distribution unlimited.

13. SUPPLEMENTARY NOTES
PAO Case Number 88ABW-2013-1345, Clearance Date 20 March 2013 . Report contains color.

14. ABSTRACT

Electromagnetic media and metamaterials have been explored in frequency regimes ranging from the acoustic to the visible domain over the past decade. Here we present the design of a focusing GRadient INdex (GRIN) lens to operate at RF frequencies that is not polarization constrained. We compare theoretical and experimental results from this lens designed to operate at X-band and fabricated using 3D printing technology. The lens with radially varying refractive index gradient was designed, optimized and analyzed by conducting full-wave simulations finite-element method based software Ansoft HFSS®. The design was fabricated and experimentally results are compared to the performance of the theoretical design.

15. SUBJECT TERMS
Electromagnetics, Rapid prototyping, Microwave Lens, Effective Medium, Metamaterials

16. SECURITY CLASSIFICATION OF:			17. LIMITATION OF ABSTRACT:	18. NUMBER OF PAGES	19a. NAME OF RESPONSIBLE PERSON (Monitor)
a. REPORT	**b. ABSTRACT**	**c. THIS PAGE**	SAR	16	Jeffery W. Allen
Unclassified	Unclassified	Unclassified			**19b. TELEPHONE NUMBER** *(Include Area Code)* N/A

Table of Contents

List of Figures

SUMMARY

Electromagnetic media and metamaterials have been explored in frequency regimes ranging from the acoustic to the visible domain over the past decade. A large part of the design, fabrication and prototyping of such materials has focused on planar structures and devices have been demonstrated primarily for certain propagation directions and/or defined polarization. Here, we present the design of a focusing GRadient INdex (GRIN) lens that operates at radio frequency (RF) frequencies and is not polarization constrained. We compare the theoretical and experimental results from this lens designed to operate at X-band and fabricated using three dimensional (3D) printing technology to implement the effective medium. The lens with radially varying refractive index gradient was designed, optimized and analyzed by conducting full-wave simulations finite-element method based software. The permittivity was estimated by effective medium theory and calculated using HFSS®. The optimized design was used to fabricate the GRIN lens with isotropic, inhomogenous dielectric material. The refractive index was designed to match the theoretical results using mixing ratio of air/voids and a polymer. Further, we used the refractive index profile to predict the rays' trajectories and focus length to compare them to those predicted by the finite element method (FEM) simulations. The field distributions were also analyzed to compare performance of the theoretical design to the fabricated lens and were found to be in good agreement with each other.

1 INTRODUCTION

Engineered electromagnetic materials and metamaterials have been researched in recent literature to explore devices that enable access to electromagnetic properties that are not available in nature. This new class of devices can not only open the door to new functionality but also be effectively utilized to improve the overall performance of existing systems with respect to electromagnetic performance, cost, size, weight and repeatability. The most important implication of engineered electromagnetic materials is the fact that they allow a designer access to materials with spatially varying anisotropic electromagnetic properties (permittivity, ε and permeability, μ) that are specified to match a given application [1, 2]. However, it should be noted that while metamaterials offer a set of viable solutions to modify the behavior of waves in a media, there are also a wide range of other engineered electromagnetic materials such as graded dielectrics that can be used to design practical media that is easily fabricated and offers attractive properties in terms of manipulating wave propagation [3]. Both graded dielectrics and metamaterial have been explored in the past using both simulation studies and practical demonstrations [4-6]. One example of such structures is the double-fishnet that has been used to fabricate 3D metamaterial structures [7].

In this work, we focus on the design, fabrication, and characterization of a 3D metamaterial implementation of a GRIN lens. Some examples of lenses with gradient refractive index distribution [8] include the radial gradient in the cylindrical coordinates (Wood lens), radial gradient in the spherical coordinates (Maxwell fish-eye-shaped and the Luneburg lens), and planar gradient lens [9]. An important application of such lenses in the microwave regime is in antenna systems with high directivity for beam scanning [10]. These lenses can be used to manipulate wave propagation such as convert spherical waves into flat plane waves. In the microwave bands, GRIN lenses are often made of polystyrene [11]. Currently focusing lenses with homogenous refractive index are curved. Their size and weight can also make them prohibitive in certain applications such as air-borne systems where these constraints are crucial to efficient operation. These issues can be addressed by designing a lens based on metamaterial structures and manufactured with 3D printing. We choose to use a metamaterial based design approach to improve on existing refractive index only based designs to mitigate some of the scattering and weight issues of existing components. It also allows us the freedom to manipulate the electromagnetic waves while maintaining performance.

2   DESIGN AND SIMULATION OF THE GRIN LENS

We present the design of a gradient index lens with an operational frequency of 12GHz capable of focusing a uniform plane wave to a point outside the lens. We begin with the Eikonal limit approach, to provide a first estimate for the performance of a metamaterial planar GRIN lens. This is studied using geometric optics such that an appropriate gradient refractive index distribution can be determined, that creates a focus at the desired length. The thickness of the lens is denoted by 't' and the focus is located at F(0,-f) where 'f' is the focal length. The refractive index distribution can be given by a function, n(x), that describes the gradient distribution in the x-direction but remain invariant in the z-direction. D is the radial extent of the lens, O is the origin and T is the dimension in the direction of propagation. A plane wave that consists of parallel rays incident on the top surface undergoes multiple refractions through the lens and converges into a focus at F. Conversely, if a divergent beam is incident on the bottom surface, it gets converted to a plane wave as it emerges from the top surface. The optical path of an arbitrary ray located at 'x' can be written as:

$$p(x) = \frac{\sqrt{f^2 + x^2} + n(x)t}{\lambda_0} \tag{1}$$

For the rays to all converge to a single focal point, the optical path lengths of arbitrary off-axis rays should equal to those passing exactly at the optical axis. This can be expressed mathematically through the refractive index distribution as shown in Equation 2.

$$n(x) = n_0 - \frac{1}{t}\left[\sqrt{f^2 + x^2} - f\right] \tag{2}$$

The optical paths of the rays are curvilinear but can be approximated to linear paths for a very thin lens. The lens can also convert cylindrical waves emitted by the line source placed at the focus into plane waves after passing through the lens. The lens we designed has a thickness of 4.5cm and radius of 11cm with a focal length of 25cm.
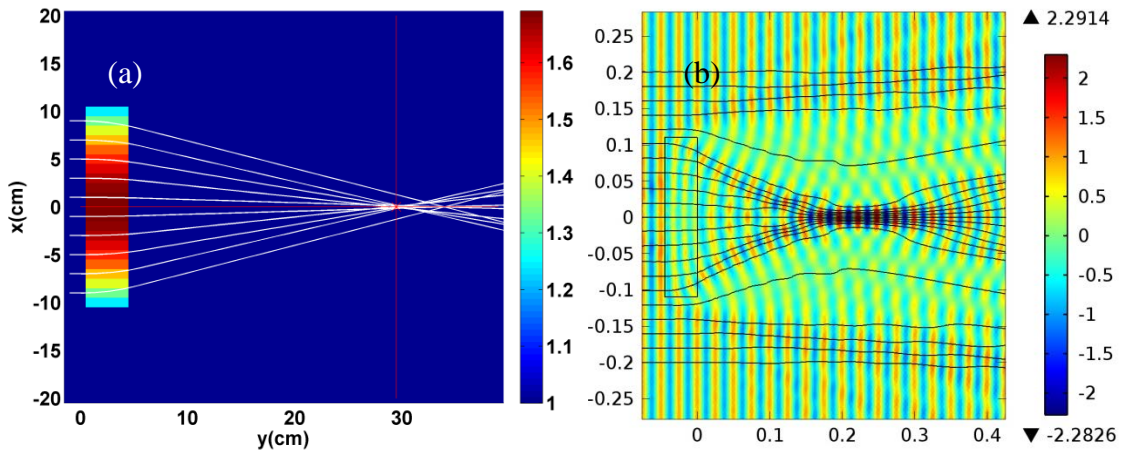

Figure 1: (a) Ray paths calculated for a given focus and refractive index profile using ray tracing; (b) Focus is verified using time average power full wave electromagnetic 2D Comsol simulation of lens using refractive index profile described by Equation (2) (not individual unit cells). The electric field is also plotted and shown by the rainbow map with associated color bar on the right

In contrast to lenses designed for operation in the optical regime, where lens size is many magnitudes larger than the wavelength, lenses that operate at RF wavelengths are physically only a few times larger than the wavelength. Therefore, approximations such as Eikonal limit predictions that can be made at optical wavelengths are not entirely accurate in the RF regime [12]. In order to fully describe the lens, full wave electromagnetic analysis must be carried out that takes into account near-field effects such as scattering and diffraction. Since this analysis is complex and time consuming, approximations are usually used at first to gain insight into the basic function of such devices. The solutions obtained from these simple methods can then be refined using more rigorous methods. To this end, we use first order approximations using ray tracing and two dimensional (2D) simulations which are followed with full 3D models and measured results.

We begin with the refractive index profile was used in a Matlab® program to predict the rays' trajectories and focal length. The program takes into consideration the differential index gradient and uses the method described by Sharma et al [13] to predict ray path and convergence point/focus. The simulation results for focal length are compared to those predicted by the Equation (2) and found to be comparable at 25 cm. While the ray tracing provides a good estimate of the properties of the lens, these are not exact estimates. This is because at microwave frequencies the size of the lens is comparable to the operational wavelength and thus challenges the Eikonal limit. A near-field solution has to be considered for more exact results. We compare the focal length calculated by this approach to that determined using full wave 2D simulations of the lens to elucidate this difference. The basic lens profile is modeled using finite element based simulations in Comsol® to analyze the power distribution and ray trajectories are estimated using time average power. These results are plotted in Figure 1 and the focus is found to be at ~23cm. The electric field profile is also plotted using a rainbow map and overlaid on the power flow lines. It follows the same pattern as the power as expected. Further, it should be noted at this point that 2D simulations of electric field have a $\left(1/\sqrt{r}\right)$ dependence while those in 3D have a $(1/r)$ dependence which creates discrepancies in the results. The 2D models simulated in Comsol® can be modified to a 3D case using the appropriate function with radial and angular dependence but those simulations were not performed due to computational overhead and instead the actual 3D lens structure with units cells was simulated to present a more complete picture. These 3D simulations were performed using HFSS® and results are presented later in the paper.

Once the refractive index profile is verified to have the required focal length at 12GHz, the next step is to design the electromagnetic media that will be used to fabricate the lens. This process begins with the design of the unit cells. The unit cell geometry chosen for this lens was a square dielectric with a void in the center (refer Figure 2(a)). The material properties of the dielectric used by the 3D printer are $\varepsilon=2.86$ in the frequency regime of interest. We begin with a structure where the dimensions are approximated using the Maxwell-Garnett (MG) formula. The MG formula is well suited to discrete inclusion mixtures which occur in nature and is easily extended to engineered materials with disparate unit cells that act in unison to produce the behavior of an effective medium. This formula works best for small filling fractions and low material contrasts where the material properties of inclusions do not differ much from the background material. Therefore this approximation will not be valid for the extreme case of a solid dielectric block and dielectric blocks with very small holes. It should also be noted that MG formula is only valid for wavelengths which are long in comparison with the periodicity of the unit cells in the engineered medium [14-16]. Since our unit cell size falls well within this constraint we can use the MG

formula for most of the cells noting that some cells will be excluded based on filling fraction constraints and material polarization effects.

With this initial guess of a partially filled/void unit cell, we conduct parametric studies using standard material retrieval processes conducted using HFSS® to determine the exact size of the voids that will give us the required index at each point. The refractive index vs. void volume that results from the extraction is calculated and plotted. Twenty five different unit cells were simulated varying the volume of the void from 0 to 97.3 mm^3. This data was fitted to find an equation that represented the curve shown in Figure 2(b) and was used to programmatically draw each of the over 10,000 unit cells in the lens that make up the effective medium. Finally, the refractive index of the lens vs. radius (Figure 2(c)) was used to determine the placement of the designed unit cells.
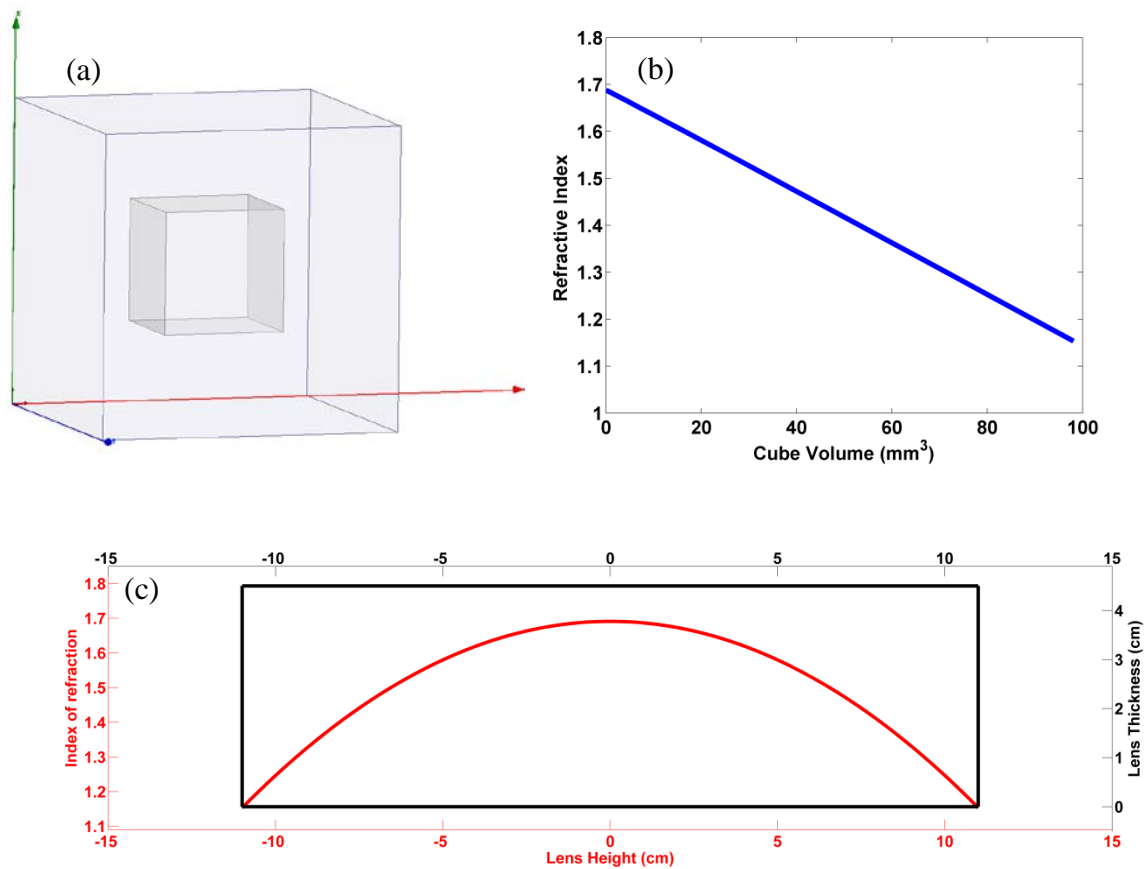

Figure 2: (a) Structure of simulated unit cell, inner dark grey box represents void; (b) Refractive index of a single unit cell vs. volume of the void in the cell. This helps define geometry of the cell needed for a given refractive index; (c) Plot of refractive index of the lens vs. radial distance. Lens height is plotted on the right as a reference

Full wave electromagnetic simulations based on FEM using commercial software HFSS® are used to explore and verify different unit cell designs that give the requisite refractive index. The material parameters of the effective medium are calculated from the retrieved S-parameters of the unit cells simulated in HFSS® in the usual manner [17,18]. The bounds of the studies are defined by the extremes of the unit cell design with no hole at one extreme (solid dielectric block unit cell) and the other extreme with the largest hole dimension dictated by the minimum thickness that can be fabricated depending on the strength of the chosen dielectric material and

the printer resolution (hollow unit cell with thin walls). We concluded our simulation studies by conducting 3D full wave electromagnetic simulations of the entire lens with actual unit cell dimensions and material parameters that were then used to fabricate the experimental device. The dimensions of the computational domain are 47cm in the *x*-direction and 30cm in the *y* and *z* directions. Radiation boundary conditions are used with an excitation of a uniform plane wave traveling in the *x* direction. The back face of the lens is centered at coordinates [0,0,0] and the lens extends 4.5cm in the negative *x* direction. The front face of the lens where the plane wave is incident is located at *x*=-4.5cm.
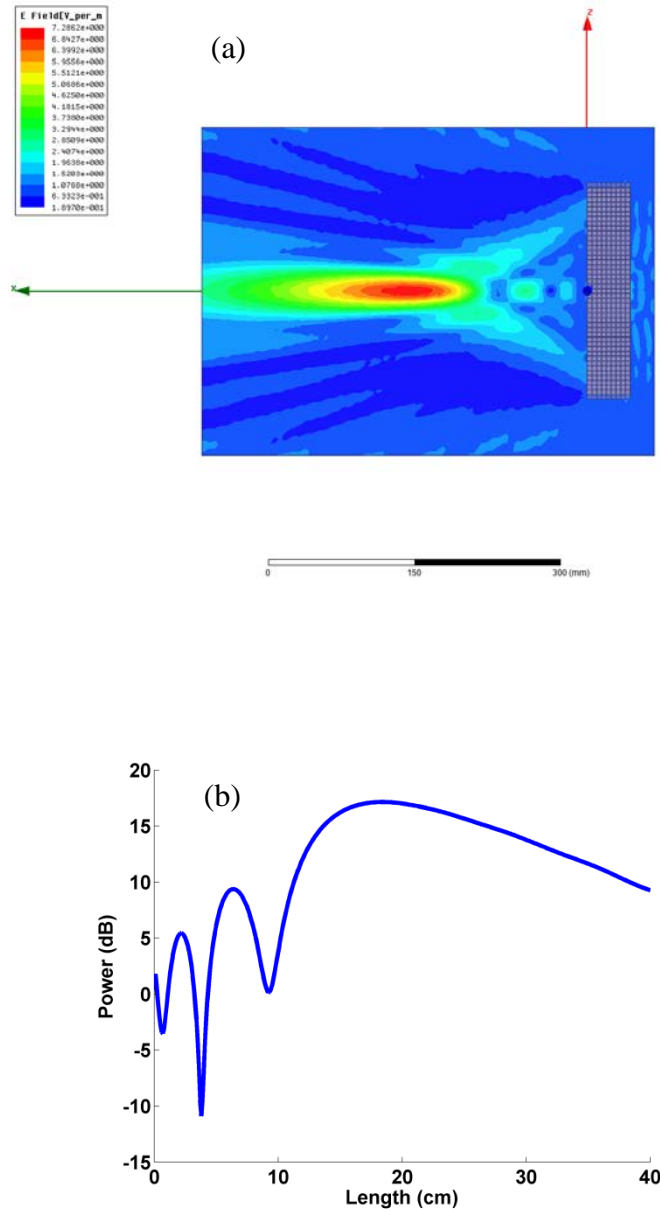

Figure 3: (a) Results of full 3D electromagnetic simulation of a homogenized 3D lens (with actual unit cells) carried out in HFSS®: Electric field shows focus at location of 18.5cm; (b) The power is plotted along the x-axis (along the center of the lens, from the face outwards) shows focus where magnitude is maximum

These simulations will be a more accurate representation of a real lens and closer to the measured data since all near-field effects are accounted for. Figure 3(a) shows the magnitude of the electric field in the *xz*-plane for a uniform incident plane wave with *z*-polarization. The magnitude of the electric field was then plotted along the *x*-axis, which also represents the median of the lens. This line graph is shown in Figure 3(b). The maximum of the electric field shows where the plane wave converges and the electric field is most concentrated and thus represents the focus of the lens. This is approximately at ~18.5 cm. As explained earlier, this is different from the focal length predicted by the 2D model but closer to the result measured in the fabricated laboratory prototype of the lens.

3 FABRICATION AND CHARACTERIZATION OF THE LENS

We used a 3D rapid prototyping printer to fabricate the GRIN lens shown in Figure 4. 3D printers can be used to print a diverse set of materials from dielectrics to metals. The materials can be used either individually or in combination (mixed during fabrication) to obtain anisotropic permittivity and permeability values with a range wider than the basic materials used in their neat form [19, 20]. We can also further enhance this range of available material parameters through careful design of geometric features in the unit cells. For example, to lower the limit on available refractive index range, we included holes/voids in this lens design. Since these voids can be defined in the computer-aided design (CAD) file, the printing is seamless and does not require an additional milling step used in conventional processes.The lens was measured on a modified microwave Gaussian beam system. The system is used to fully illuminate the lens with a wave and measure the performance of the manufactured lens. The measurement system emits a Gaussian like wave that does not have uniform amplitude or phase. This has to be accounted for because it has a large effect on the output of the lens. The electric field is measured down the centerline of the lens from 10cm to 40cm from the back face of the lens in a similar fashion to the data obtained in the simulations earlier. The incident wave was modeled as a Gaussian beam with a phase center of 25cm and an aperture radius where the power decreased to e^{-1} of 6.5cm to closely match the wave used to illuminate the lens in the experimental measurements. After taking into consideration the amplitude taper and phase variation of the incident wave in the computational electromagnetic simulations, the measured data compares favorably to the simulations (refer to Figure 5 below).
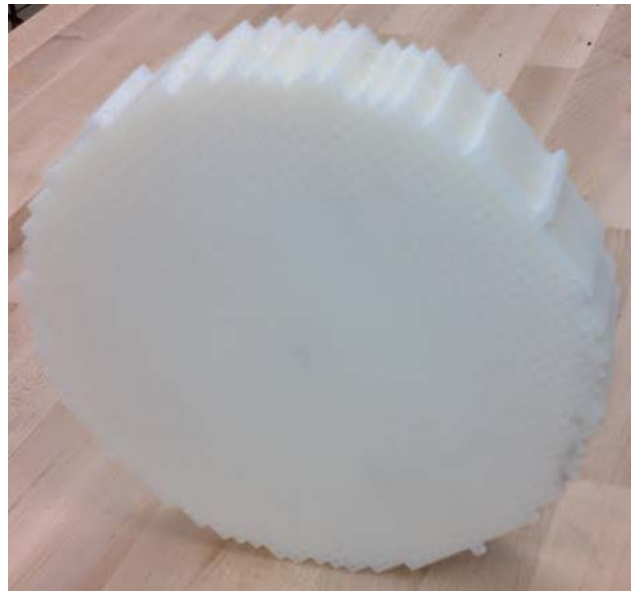

Figure 4: GRIN lens fabricated using 3D printer. The fill factor decreases radially outwards and the voids are visible in the unit cells as you approach the periphery of the lens

4   DISCUSSIONS AND CONCLUSIONS

Microwave lenses such as GRIN lenses are used in a variety of applications such as electromagnetic wave collection and imaging. These lenses are major contributors to system size, weight and cost which forces tradeoffs between system parameters such as focal length, field of view, resolution, bandwidth, reflectivity, and range. We choose to use a metamaterial based design approach to improve on existing refractive index only based designs and mitigate some of the scattering and size issues of existing components. It also allows us the freedom to manipulate the electromagnetic waves while maintaining performance. The possibility of partial/full metallization further increases the range of constitutive parameters available for the designs. The 3D printing approach was chosen to show how such methods can be used to efficiently and accurately fabricate such devices and electromagnetic materials. This allows for building truly 3D electromagnetic structures as opposed to stacked layer approaches which gives us the freedom to leverage geometrical anisotropy as well as 3D material variation in our designs which in turn increase the degrees of freedom available to optimize the unit cells (and thus material parameters) for a given application.
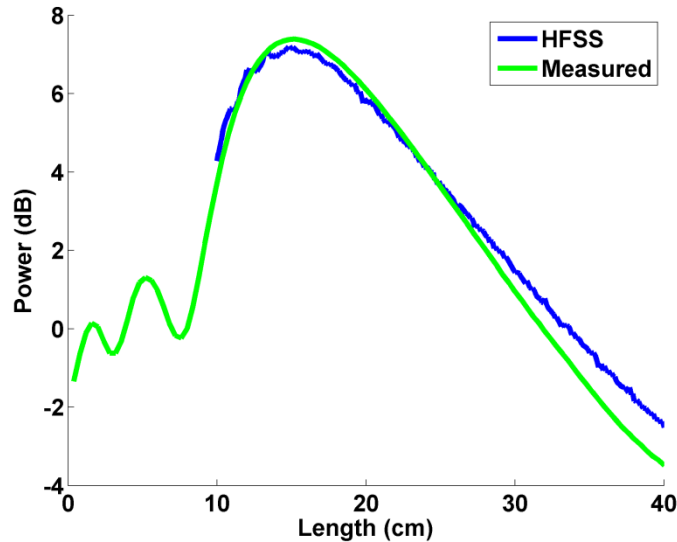

Figure 5: Comparison of the simulated data to the measured data of power down the centerline of the lens. (a) Simulated in HFSS®, (b) Experimentally measured

In conclusion, we have studied the designed and demonstrated a microwave GRIN lens that operates at 12GHz. We used theoretical modeling and full wave 2D/3D electromagnetic simulations to study the behavior of the device and also design the individual unit cells that constitute the homogenized medium used in the fabrication of the lens. Finally, we used this design to fabricate the lens using a 3D rapid prototyping method which fully automated the process and eliminated post-processing steps such as milling from the design. The fabricated lens was then experimentally measured and characterized for field distribution and focal length. The theoretical models and experimental results were found to be comparable. We expect that demonstration of such devices will pave the way for quick turnaround demonstrations of practical microwave devices.

5   REFERENCES

[1] N. Engheta, R. W. Ziolkowski, "Electromagnetic Metamaterials: Physics and Engineering Explorations," Wiley IEEE Press, (2006)

[2] W. Cai, V. Shalaev, "Optical Metamaterials: Fundamentals and Applications," Springer, (2009)

[3] F. Capolino, E. N. Economou, T. Koschny , C. M. Soukoulis, and M. Kafesaki, "Designing One-, Two-, and Three-Dimensional Left-Handed Materials," Theory and Phenomena of Metamaterials CRC Press, (2009)

[4] W. E. Kock, "Metallic delay lenses," Bell System Technical Journal 27, 58 (1948)

[5] W. E. Kock, "Metal-Lens Antennas," Proceedings of the IRE 34, 828-836 (1946)

[6] R. W. Corkum, "Isotropic artificial dielectric," Proceedings of the IRE 40, 574–587 (1952)

[7] C.M. Soukoulis, M. Wegener, "Past achievements and future challenges in the development of three-dimensional photonic metamaterials," Nature Photonics 5, 523-530 (2011)

[8] D. R. Smith, J. J. Mock, A. F. Starr, and D. Schurig, "Gradient index metamaterials," Physical Review E 71, 036609 (2005)

[9] I. M. Ehrenberg, S, E. Sarma, and B-I Wu "A three-dimensional self-supporting low loss microwave lens with a negative refractive index," Journal of Applied Physics 112, 073114 (2012)

[10] H. Chen, B-I Wu, L. Ran, T. M. Grzegorczyk, and J. A. Kong "Controllable left-handed metamaterial and its application to a steerable antenna," Applied Physics Letters 89, 053509-053509 (2006)

[11] A. Carswell and C. Richard, "Focal Properties of Microwave Lenses with Small F-Numbers," Applied Optics 10, 346-357 (1971)

[12] M. Born, E. Wolf, "Principles of Optics," Pergamon, (1964)

[13] A. Sharma, A. Ghatak, "Ray tracing in gradient-index lenses: computation of ray-surface intersection," Applied Optics, 25, 3409-3412 (1986)

[14] G. Milton, "The theory of composites," Cambridge: Cambridge University Press, (2002)

[15] P. Mallet, C. A. Guerin, and A. Sentenac, "Maxwell-Garnett mixing rule in the presence of multiple scattering: Derivation and accuracy," Physical Review B 72, 014205 (2005)

[16] S. Zouhdi, A. Sihvola, and A. P. Vinogradov, "Metamaterials and Plasmonics: Fundamentals, Modelling, Applications," Springer Netherlands, (2009)

[17] D.R. Smith, D. C. Vier, T. Koschny and C. M. Soukoulis, "Electromagnetic parameter retrieval from inhomogeneous metamaterials," Physical Review E 71, 036617 (2005)

[18] D. R. Smith, J. B. Pendry, "Homogenization of metamaterials by field averaging," JOSA B 23, 391-403 (2006)

[19] P. C. Joshi, R.R. Dehoff, C.E. Duty, W.H. Peter, R.D. Ott, L.J. Love, and C.A. Blue, "Direct digital additive manufacturing technologies: Path towards hybrid integration," Future of Instrumentation International Workshop, (2012)

[20] M. Vaezi, H. Seitz , S. Yang "A review on 3D micro-additive manufacturing technologies," International Journal of Advanced Manufacturing, 1-34 (2012)

LIST OF ACRONYMS, ABBREVIATIONS, AND SYMBOLS

ACRONYM	DESCRIPTION
2D	two dimensional
3D	three dimensional
AFRL	Air Force Research Laboratory
CAD	computer-aided design
FEM	finite element method
GHz	gigahertz
GRIN	gradient index
MG	Maxwell-Garnett
RF	radio frequency
ε	permittivity
f	focal length
λ_0	free space wavelength
μ	permeability
n	index of refraction
p	optical path
r	radius
t	lens thickness